Vol. 724: 47–65, 2023
https://doi.org/10.3354/meps14448

MARINE ECOLOGY PROGRESS SERIES
Mar Ecol Prog Ser

Published December 7

Carbon budgets of copepod communities in the northern Humboldt Current System off Peru

Anna Schukat[1,*], Maya Bode-Dalby[1], Jana C. Massing[2,3], Wilhelm Hagen[1], Holger Auel[1]

[1]Universität Bremen, BreMarE — Bremen Marine Ecology, Marine Zoology, 28359 Bremen, Germany
[2]Helmholtz Institute for Functional Marine Biodiversity at the University of Oldenburg (HIFMB), 26129 Oldenburg, Germany
[3]Alfred Wegener Institute, Helmholtz Centre for Polar and Marine Research, 27570 Bremerhaven, Germany

ABSTRACT: Abundance, biomass and respiration rates of dominant medium- to larger-sized copepod species (ML class) from the upwelling system off Peru (8.5–16° S) were determined along with their carbon ingestion and egestion rates. Small copepods (S class) were included for comparisons of community rates. Overall, abundance/biomass was highest in the upper 50 m and decreased with depth and thus also community ingestion and egestion. Ingestion of the ML class (0–50 m) in shelf regions (14–515 mg C m^{-2} d^{-1}) was lower in the south compared to the north and central study areas, while their offshore ingestion (11–502 mg C m^{-2} d^{-1}) was comparable across regions (8.5–16° S). Ingestion rates (0–50 m) of the S class were in a range similar to those of the ML class in shelf regions (100–417 mg C m^{-2} d^{-1}) but were higher offshore (177–932 mg C m^{-2} d^{-1}). *Calanus chilensis* and the S class contributed most to total ingestion in the north, while in the south, *Centropages brachiatus* had the highest community ingestion aside from the S class. Egestion varied from 3–155 mg C m^{-2} d^{-1} for the ML class and 30–280 mg C m^{-2} d^{-1} for the S class. The high community rates highlight the crucial role of both size classes for carbon budgets in the northern Humboldt Current System off Peru and indicate that the ML class may enhance passive vertical carbon flux, whereas the S class may support carbon remineralization rates in surface waters.

KEY WORDS: Upwelling · Biological carbon pump · Consumption rate · Calanoid copepods

1. INTRODUCTION

The Humboldt Current System (HCS) is one of the most productive regions in the world's oceans and plays an important role in the ocean's carbon cycle (Carr 2002, Vargas & González 2004). Along the coast of northern-central Peru, upwelling is strong and occurs permanently throughout the year (Montecino & Lange 2009). High production rates caused by the strong upwelling support the world's largest single-species fishery on Peruvian anchovy off Peru (Bertrand et al. 2004, Chavez et al. 2008). Copepods typically comprise between ~70 and 90% of the mesozooplankton community in terms of abundance in coastal upwelling systems (Hansen et al. 2005, Criales-Hernández et al. 2008) and may play a crucial role in the cycling of organic matter, e.g. via molted exoskeletons, fecal pellets and respiration processes. Respiration rates are an indicator of a species' metabolic activity and provide robust assessments of metabolic demands and energy expenditures (Ikeda et al. 2000, Brown et al. 2004, Hernández-León & Ikeda 2005a). Additionally, oxygen consumption rates are commonly used to calculate ingestion rates by applying an energy budget approach, with an assumed respiratory quotient (RQ) as well as assumed efficiencies for growth and assimilation (Pakhomov et al. 1999, Ikeda et al. 2000, Hernández-León & Ikeda 2005a). Species-specific information on respiration and ingestion rates of

*Corresponding author: schukat@uni-bremen.de

copepods in the HCS off Peru and Chile is still limited (Dagg et al. 1980, Castro et al. 1991, Vargas & González 2004). For the calculation of realistic carbon budgets of the HCS, additional data on metabolic demands and carbon consumption of dominant copepod species are needed. Furthermore, to calculate the contribution of different copepod species to carbon export fluxes, information on their abundance and biomass distribution as well as species-specific vertical migration behavior is crucial.

The active transport of carbon by species that undergo diel vertical migration (DVM) and the passive transport of sinking particles such as fecal pellets are the 2 major pathways for zooplankton-mediated carbon export from the surface to deeper layers of the ocean (Longhurst et al. 1990, Steinberg et al. 2008). Diel vertical migrants feed at the surface during the night and descend to deeper layers during daytime, where a certain amount of the food is defecated, respired and excreted. The global average of active carbon export by migrating zooplankton is only 10%, while passive export accounts for 70% of the total biological carbon pump export (Nowicki et al. 2022). However, active flux can locally dominate or reach magnitudes similar to those of passive fluxes (Steinberg & Landry 2017), especially in productive regions such as the Canary Current (Hernández-León et al. 2019). The passive export flux at 100 m in the HCS off Chile (González et al. 2000, 2007) and the Southern California Bight (Landry et al. 1994) as well as in oligotrophic oceanic regions in the Pacific and Atlantic (Boyd et al. 2008) mostly consists of fecal material of zooplankton. In addition, appendicularian houses and carcasses can also constitute an important component of passive fluxes (Vargas et al. 2002, Alldredge 2005). The downward carbon flux mediated by zooplankton can be altered in regions with an oxygen minimum zone (OMZ) since low oxygen levels in the water column influence the vertical distribution and DVM behavior of zooplankton species (Judkins 1980, Escribano 2006, Kiko & Hauss 2019).

The OMZ in the HCS is much more pronounced in its vertical extent and low oxygen levels compared to other eastern boundary upwelling systems, e.g. the Benguela and Canary Currents (Chavez & Messié 2009). Along the Peruvian coast, an almost anoxic core expands from ~50–100 m down to 500–600 m (Fuenzalida et al. 2009). Due to the presence of this intense OMZ that extends from very shallow depths, many prevailing species such as the copepods *Calanus chilensis* and *Centropages brachiatus* remain in the upper 50–60 m during day and night (Boyd et al. 1980, Escribano & Hidalgo 2000, Criales-Hernández et al. 2008, Morales et al. 2010, Schukat et al. 2021). In contrast, large-scale migrations from the surface layer into the OMZ to depths below 200 m are performed by the larger-sized copepod *Eucalanus inermis* (Tutasi & Escribano 2020) and several euphausiid species such as *Euphausia mucronata* and *Nematoscelis gracilis* (Antezana 2009). Vertical distribution patterns of *E. inermis* are variable, including normal and inverse DVM from above 100 m to below 300 or 500 m (Tutasi & Escribano 2020) or smaller-scale migrations (<100 m distance) within the OMZ (Hidalgo et al. 2005, Escribano 2006). Nevertheless, this species potentially contributes to the active carbon flux by its migrations from the surface into the OMZ. In contrast, the non-migrating copepod community can contribute to passive fluxes out of the surface layer via fecal pellets and/or to the remineralization of organic carbon, which may fuel omnivorous–detritivorous feeding and the microbial loop in surface layers.

Small copepods of the families Oithonidae, Oncaeidae, Paracalanidae and Acartiidae are highly abundant in the HCS but larger species such as *C. chilensis*, *Calanoides patagoniensis*, *E. inermis* and *C. brachiatus* also frequently occur (Boyd & Smith 1983, Peterson et al. 1988, Escribano & Hidalgo 2000, Castro et al. 2007). While several studies from the HCS off Chile have addressed the role of copepod communities in carbon budgets and export fluxes (González et al. 2000, Grunewald et al. 2002, Vargas & González 2004, Tutasi & Escribano 2020), little is known about their contribution to the carbon flow in the productive upwelling region off Peru (Dagg et al. 1980).

The objective of this study was to assess the abundance, biomass and respiration rates of dominant copepod species in the northern HCS off Peru during December 2018–January 2019 and to estimate their carbon ingestion and fecal pellet production (egestion) rates in the upper 1000 m. A broad regional range, from 8.5 to 16° S, was covered during this study, as we aimed to identify the key species contributing to the carbon flow from north to south for shelf and offshore regions off Peru. Recent studies have revealed the vital importance of small copepods to carbon budgets and export fluxes (Roura et al. 2018, Koski et al. 2020, Bode-Dalby et al. 2022). Hence, besides the dominant medium- to larger-sized copepod species, bulk samples of small-sized copepods were considered during this study to better understand the role of both size classes in the carbon cycle of the highly productive northern HCS off Peru.

2. MATERIALS AND METHODS

2.1. Sampling

Copepods were sampled with a MultiNet Midi (HydroBios: mouth opening, 0.25 m^2; mesh size, 200 µm; 5 nets) during the research cruise MSM80 with the RV 'Maria S. Merian', which took place during December 2018–January 2019. In total, 37 stations along 6 cross-shelf transects were sampled in the HCS off Peru (Fig. 1). The transects (T1–T6) were located at 8.5, 9.5, 12, 14.5, 15.3 and 16° S, with 5–7 stations each covering a depth range from 1000 m to the surface along discrete depth intervals (strata: 1000–500, 500–200, 200–100 m; 100–50 or 100–30 m; 50–0 or 30–0 m). Two 24 h stations (Stns 46 and 80) with 4 net hauls each (21:30, 03:30, 09:30 and 15:50 h local time, UTC +5) were sampled from 600–400, 400–200, 200–100, 100–50 and 50–0 m. For respiration measurements on board, live and active copepod specimens were identified to species and stage under a dissecting microscope (Leica MS5). Sorting was carried out swiftly and with special care to ensure that specimens remained in good condition. For abundance analyses, the remains of the net samples were preserved in 4% borax-buffered formaldehyde in seawater solution. Temperature, salinity and oxygen profiles were obtained for every station by using a Sea-Bird CTD (conductivity temperature depth) profiling system with Niskin bottles attached to a rosette.

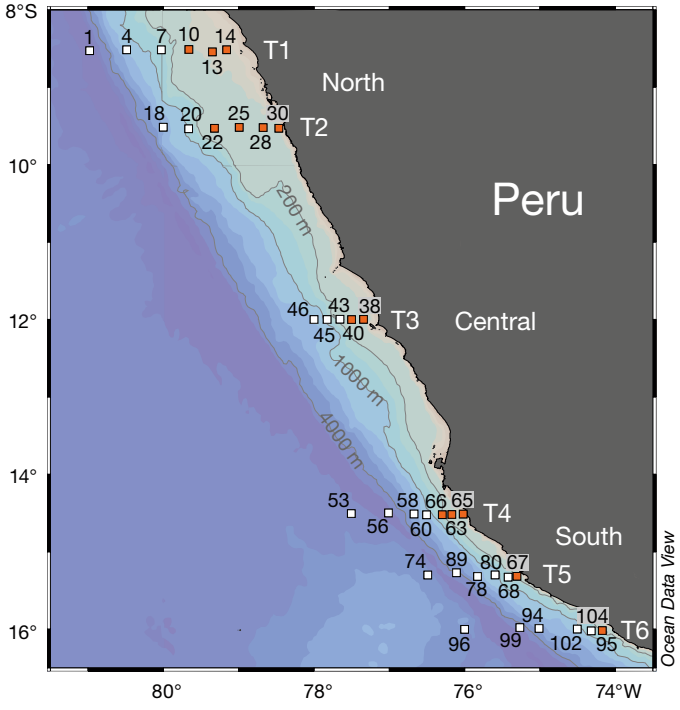

Fig. 1. Station map of transects (T1–T6) conducted during the 'Maria S. Merian' cruise in December 2018–January 2019. Color coding indicates shelf (orange) and offshore (white) stations

2.2. Biomass of copepods

All net samples were transferred to a Steedman sorting solution (0.5% propylene-phenoxetol, 5% propylene glycol and 94.5% double-distilled water; Steedman 1976) to analyze the copepod composition. Samples with high copepod densities were subdivided with a Motoda plankton splitter (Motoda 1959). All copepods with an average female prosome length (PL) of ≥1.2 mm were counted and sorted from the net samples. The dominant species were identified, staged (including copepodite stages C4–C5, female and male) and enumerated for every station. Hereafter, they are referred to as medium- to larger-sized copepods (ML class). The species- and stage-specific biomass of the ML class was calculated based on abundance and individual dry mass (DM). The DM of each ML class species was measured from either deep-frozen samples on a microbalance (Sartorius MC215) after lyophilization for 48 h or from formalin-Steedman-preserved samples. Prior to weighing, preserved individuals were briefly dipped in double-distilled water and transferred to a 96-well plate for drying at 60°C for 24 h, followed by a cooling step in a desiccator (30 min). After drying, specimens were weighed on a microbalance (Sartorius MC215) individually (for large species such as *Euchaeta* spp.) or as bulk samples with a known number of individuals (2–30), depending on the size and stage of a species.

For transects T1 and T5, small-sized copepods (S class) were included in the analysis for comparisons. This group combined all copepod species with an average female PL of <1.2 mm and comprised cyclopoid, harpacticoid and small calanoid species but also the C1–C3 stages of larger calanoid species. Copepods in the S class were enumerated in bulk and not separately for species. The bulk samples of the S class were dominated by the calanoid copepods *Acartia* spp., *Calocalanus* spp. and *Paracalanaus parvus* as well as cyclopoid species (e.g. *Hemicyclops* spp., *Oithona* spp., *Oncaea* spp.) and occasionally by copepodite stages (C1–C3) of larger calanoid species (no quantitative species composition available). Biomass of the S class was estimated by weighing a subsample (1 out of 64 to 1 out of 256) with a known number of individuals for each station and depth interval.

Losses in body DM due to formalin and Steedman preservation were considered by applying the following equation from Schukat et al. (2021): DM real (µg) = DM formalin or Steedman / 0.6251 + 5.4764 (R^2 = 0.74). All DMs of specimens taken from preserved samples were recalculated accordingly.

2.3. Respiration rates

2.3.1. Optode respirometry

Respiration rates of 6 different copepod species were measured with a 10-channel optode respirometer (PreSens Precision Sensing Oxy-10 Mini) in a temperature-controlled refrigerator. The most frequently occurring ML class species were chosen for respiration measurements to ensure sufficient specimens in good condition for replicate measurements. A total of 81 on-board respiration measurements were conducted. Temperature profiles derived from the CTD probe were used to adjust the refrigerator to the average ambient temperature. Ranges for ambient temperatures for the different depth intervals were 18–22°C (50–0 m), 16–18°C (100–50 m), 13–16°C (200–100 m), 10–13°C (500–200 m) and 6–9°C (1000–500 m). Experiments were run in gas-tight glass bottles (13–14 ml) filled with filtered (0.2 µm membrane filter) seawater to reduce bias by microbial respiration. Oxygen saturation at the beginning of experiments was between 95 and 100 %. For each run, 2 controls without animals were measured under the same conditions to correct for microbial respiration, temperature irregularities and other potential errors. The number of animals incubated per bottle was adjusted according to individual size, stage and metabolic activities measured in a previous study (Schukat et al. 2013) to avoid rapid oxygen depletion. Numbers varied between 1 and 2 individuals of large species (*Eucalanus inermis*, *Euchirella bella*, *Euchaeta rimana*), 4–6 individuals for *Aetideus armatus* and *Calanus chilensis*, and 12–15 specimens for *Centropages brachiatus*. All specimens were kept in filtered seawater for about 1 h before transferring them to the glass bottles. During the experiments, the copepods showed normal active swimming behavior and they were not fed. Hence, we consider the metabolic activity during the experiments to represent the routine metabolism of the organisms. The experiments ran in darkness for 5–9 h, depending on oxygen consumption, and oxygen concentrations were recorded every 15 s. Respiration rates were calculated from the slope of the oxygen decrease over selected time intervals. The first 60 min were not considered for the calculations to exclude impacts of raised animal activity or water temperature caused by the transfer (Kiko et al. 2016). After the experiments, all specimens were deep-frozen at −80°C for later DM determination (see Section 2.2).

2.3.2. Respiration rates calculated from body DM

In addition to the measurements taken on board via optode respirometry, more than 500 individual respiration rates were determined based on individual DM and ambient temperatures to compare both approaches and to include all dominant species and copepodite stages (C4–C6) during the cruise. Respiration calculations via DM were applied according to Bode et al. (2018), considering different activity levels and/or functional groups of copepod species. Copepods of the families Eucalanidae, Rhincalanidae and Subeucalanidae are rather sluggish and described as 'thrifty floaters' (Teuber et al. 2019), with lower metabolic rates compared to copepods with normal activity. In this study, copepods of the genus *Eucalanus* and *Subeucalanus* were included. Therefore, respiration rates were calculated separately, for (1) sluggish copepods of the families Eucalanidae and Subeucalanidae and (2) for all other copepods considered to be active, with the following equations from Bode et al. (2018):

$$\ln R_{TF}\ (\mu l\ O_2\ ind.^{-1}\ h^{-1}) = -2.180 + 0.787\ \ln(DM) + 0.131\,T \quad (1)$$

$$\ln R_{AC}\ (\mu l\ O_2\ ind.^{-1}\ h^{-1}) = -0.890 + 0.646\ \ln(DM) + 0.094\,T \quad (2)$$

where R_{TF} and R_{AC} are the individual respiration rates for eucalanid/subeucalanid and active copepods, respectively, DM represents dry mass in mg and T is the average temperature (°C) of the sampling interval. Respiration rates for each measurement and calculation are available in PANGAEA (Schukat et al. 2022).

2.4. Ingestion and egestion rates

All ingestion and egestion rates are based on respiration rates calculated via DM to include all dominant species and stages. Individual respiration rates were converted to carbon units (RC: µg C ind.$^{-1}$ d^{-1}), assuming that the respiration of 1 ml O_2 equals 0.44 mg of carbon by using a RQ of 0.82 for a mixed

diet (Auel & Werner 2003) to reflect their respiratory carbon demands. Ingestion rates of the copepods were calculated according to Ikeda & Motoda (1978), assuming an average assimilation efficiency of 70% and a gross growth efficiency of 30% (I = RC / 0.4). Egestion rates were assumed to be 30% of ingestion, regardless of species and food availability (Ikeda & Motoda 1978).

Community ingestion and egestion rates (mg C m^{-2} d^{-1}) of the ML class were calculated based on the biomass per depth stratum of each species and stage and the respective mass-specific respiration rate at ambient temperature (average temperature of the depth interval). Community rates of the S class were assessed from the bulk biomass per depth stratum at 2 transects, T1 and T5, and from calculated respiration rates from Eq. (2) for comparison.

Ingestion rates for *Euchaeta* males were not included in the calculations since ambush-feeding copepods such as *Paraeuchaeta* and *Euchaeta* have a 'sit and wait for prey' strategy, with males reducing or completely stopping feeding when mature (Yen 1988, 1991). Data on species-specific individual ingestion and egestion rates are available in PANGAEA (Schukat et al. 2022).

3. RESULTS

3.1. Hydrographic conditions

The MSM80 cruise took place during moderate upwelling consistent with sea surface temperatures (SST) at 5 m depth that never decreased below 17°C on the Peruvian shelf (Fig. 2). Generally, offshore SSTs ranged between 21 and 24°C in the northern (transects T1 and T2) and central (transect T3) study area and between 19 and 23°C in the southern study area (transects T4–T6). Coastal SST varied from 18 to 21°C at transects T1–T3, and from 17 to 19°C at transects T4–T6 (Fig. 2). The thermocline was generally located between 10 and 50 m at all transects for both shelf and offshore regions, with temperatures decreasing to 15–18°C at the northern and central transects and 12–15°C at the southern transects. Below the thermocline, temperatures dropped to about 7°C at 500 m depth.

The surface layer above the thermocline was generally well ventilated (>150 µmol O_2 l^{-1}), while dissolved oxygen concentrations below the thermocline decreased sharply, generating an OMZ with hypoxic levels of ≤45 µmol O_2 l^{-1} at all transects (Fig. 2). In the northern transects (T1 and T2), the OMZ extended from around 50 to 900 m depth at oceanic regions, with near-anoxic conditions of <2 µmol O_2 l^{-1} between 200 and 600 m. Oxygen levels along the northern coast were generally above 45 µmol O_2 l^{-1} throughout the water column. The OMZ was shallower at the central Peruvian shelf break and oceanic area (transect T3), where it extended from ~30 m to the seafloor at the shelf break and to 900 m offshore, with almost zero oxygen from about 100 to 500 m. Along the coast at transect T3, the OMZ extended from close to the surface (at ~10 m) to the seafloor, with anoxic conditions from ~100 m downwards. On the southern Peruvian shelf break and offshore (transects T4–T6), the OMZ stretched from 30 to 40 m down to about 950 m depth, with an anoxic core from ~80 to 450 m. The OMZ along the southern coast extended from 15 or 20 m to the seafloor, with oxygen depletion from about 45 m onwards (Fig. 2).

3.2. Biomass distribution and species composition of copepods

The vertical trend in biomass distribution of the ML class at all stations was comparable during all times of the day, i.e. dawn, day, dusk and night (Fig. 2). At the two 24 h stations (Stns 46 and 80), biomass was concentrated in the upper 50 m during both day and night.

The highest biomass of the ML class always occurred from 0 to 30 or 50 m throughout the sampling area; at only one station (Stn 40) was the biomass maximum located between 50 and 100 m (Fig. 2). Surface biomass (0–30 or 0–50 m) at the northern transects (T1 and T2) ranged from 7 mg DM m^{-3} (respective abundance: 48 ind. m^{-3}) at Stn 22 to 64 mg DM m^{-3} (300 ind. m^{-3}) at Stn 13. Similar variations in surface biomass, from 6 mg DM m^{-3} (218 ind. m^{-3}) at Stn 40 to 77 mg DM m^{-3} (932 ind. m^{-3}) at Stn 43, occurred at the central transect (T3). At the southern transects (T4–T6), surface biomass was generally lower than at the northern and central transects, ranging from <1 mg DM m^{-3} (Stns 63 and 65) to 58 mg DM m^{-3} (1158 ind. m^{-3}) at Stn 74 (Fig. 2).

A pronounced decrease in biomass of the ML class with depth occurred at transects T4–T6. This decrease in biomass coincided with a sharp decrease in oxygen concentrations in the south, forming almost anoxic conditions from ~30–40 m downwards (Fig. 2). In contrast, in the northern and central transects, the anoxic core of the OMZ was shifted to deeper water layers (~100–200 m downwards) and the ML class occurred more frequently below 50 m

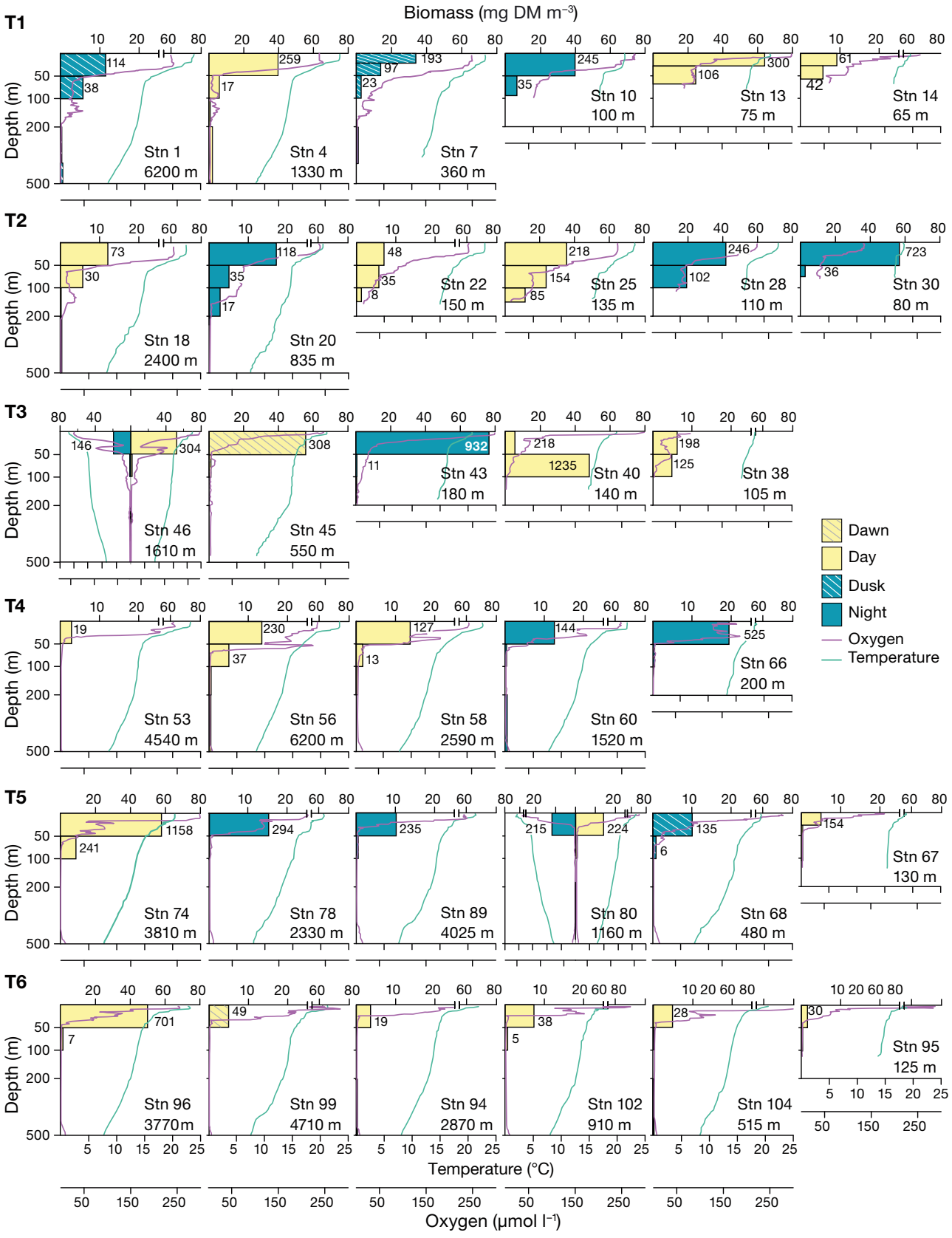

Fig. 2. Vertical biomass distribution of the ML class copepods, also showing abundance values (no. of ind. m^{-3}) next to the bars for all transects (T1–T6). Time of sampling is indicated by the color code of bars. Day and night sampling was conducted at Stns 46 and 80. Oxygen and temperature profiles as well as bottom depth (below station labels) are presented for all stations. Biomass at shelf Stns 63 and 65 (T4) and below 500 m was <1 mg DM m^{-3} (not shown). Note the scale break in some *x*-axes for biomass. See Fig. 1 for transect details

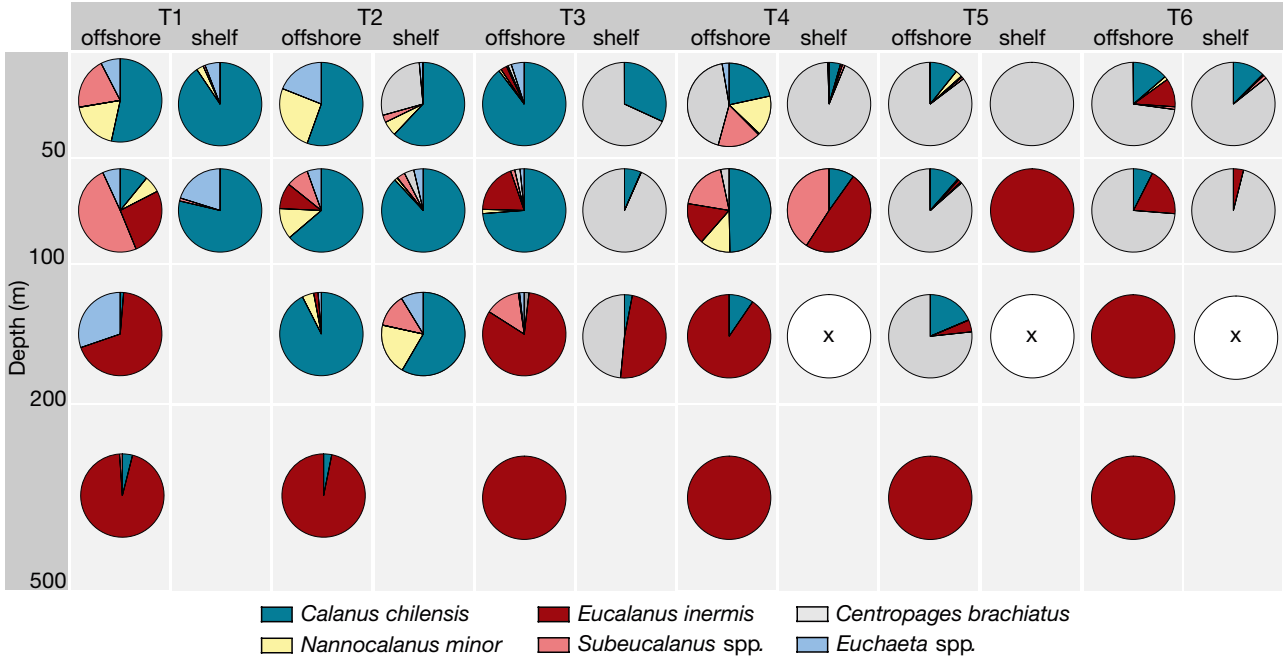

Fig. 3. Species composition of the ML class copepods per depth interval for offshore and shelf regions for every transect (T1–T6). × signifies no occurrence of these species in that depth interval. See Fig. 1 for transect details

depth, reaching biomasses of up to 48 mg DM m^{-3} (1235 ind. m^{-3}) from 50–100 m (Stn 40) and 3 mg DM m^{-3} (17 ind. m^{-3}) below 100 m (Stn 20).

Differences in the relationship between biomass and abundance are caused by the species composition, which differed for the ML class from north to south and with depth. For visualization of species composition of the ML class, all offshore and shelf stations were combined for each transect (Fig. 3). *Calanus chilensis* was the most abundant species within the ML class from 0–100 m at offshore regions (11–64 % of total abundance [TA]) and especially at shelf regions (62–91 % TA) in the north at transects T1 and T2 (Fig. 3). At these transects, *Nannocalanus minor* (7–26 % TA), *Euchaeta* spp. (6–19 % TA) and *Subeucalanus* spp. (0–49 % TA) also contributed to TA at the offshore regions in the upper 100 m. In contrast to the north, *Centropages brachiatus* became the most abundant species in the south at transects T4–T6, especially in the upper 50 m at shelf regions (86–100 % TA). In general, *Eucalanus inermis* was the dominant species below 100 m depth throughout the sampling area and almost exclusively constituted the abundance of the ML class at 200–500 m. Furthermore, it was the only species occurring at the depth interval of 500–1000 m at a few stations.

The vertical biomass distribution of the S class was comparable to the ML class, with biomass maxima in the surface layer and a decrease with depth (Fig. 4). In contrast to the ML class, the biomass of the S class was higher in the south at transect T5 than in the North at transect T1, with surface biomass ranging from 5 to 19 mg DM m^{-3} (865–2833 ind. m^{-3}) at transect T1 and from 8 to 76 mg DM m^{-3} (1313–7603 ind. m^{-3}) at transect T5. Similar to the ML class, no differences in the vertical biomass distribution were evident between day and night for the S class (Fig. 4).

3.3. Respiration rates of copepods

Individual DMs of ML class copepods ranged from 12 ± 1 µg DM $ind.^{-1}$ (±SD) for copepodite stage C4 of *C. brachiatus* to 1117 ± 118 µg DM $ind.^{-1}$ for *Euchirella bella* females (Table 1). Average DM of bulk samples of the S class ranged from 3 to 10 µg DM $ind.^{-1}$ depending on species composition. The overall mean DM of the S class was 7 ± 2 µg DM $ind.^{-1}$ (Table 1).

Respiration rates for the same species and stages were not significantly different between regions (i.e. offshore and shelf or north, central and south) but they differed significantly among depth intervals due to the lower temperatures at depth (1-way ANOVA, Kruskal-Wallis and Dunn's post hoc test). Table 1 summarizes the directly measured and calculated

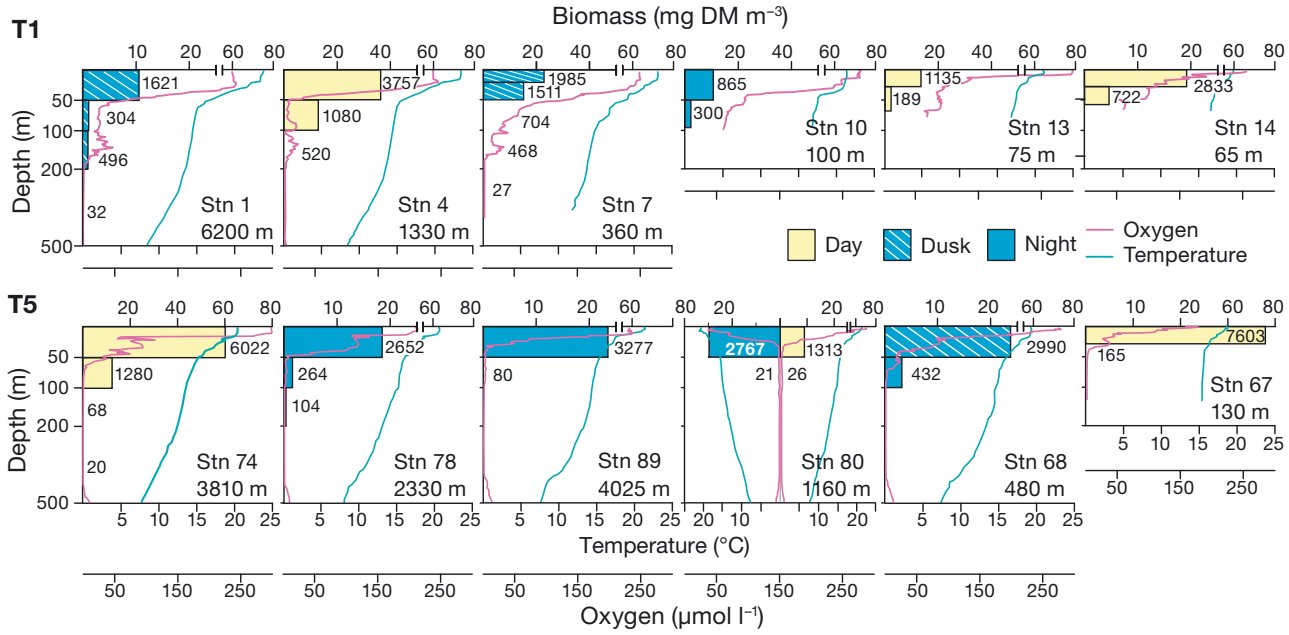

Fig. 4. Vertical biomass distribution of the S class copepods, also showing abundance values (no. of ind. m^{-3}) next to the bars for transects T1 and T5. Time of sampling is indicated by the color code of bars. Day and night sampling was conducted at Stn 80. Oxygen and temperature profiles as well as bottom depth (below station labels) are presented for all stations. Biomass below 500 m was <1 mg DM m^{-3} (not shown). Note the scale break in some *x*-axes for biomass. See Fig. 1 for transect details

respiration rates for different developmental stages and depth intervals of the dominant copepods.

Hereafter, respiration rates refer to a temperature of 20°C unless stated otherwise. Individual respiration rates (IRR) measured via optode respirometry ranged from 2.2/4.9 µl O_2 ind.$^{-1}$ d^{-1} (1.0/2.2 µg C ind.$^{-1}$ d^{-1}) for female *Aetideus armatus* to 69.3 ± 4.7 µl O_2 ind.$^{-1}$ d^{-1} (30.5 ± 2.1 µg C ind.$^{-1}$ d^{-1}) for female *E. bella* (Table 1). The measured respiration rates were significantly correlated with the calculated rates for the respective DM of a species (Spearman's correlation, r = 0.730, p < 0.001) when the heaviest species (*E. bella*, >1000 µg DM ind.$^{-1}$) was excluded from the regression analysis (Fig. 5). Measured *E. bella* respiration rates were only about half of the values expected from the body-mass–respiration rate regression (Table 1).

Respiration rates calculated via DM are presented to compare all dominant species during the cruise (Table 1). The S class had an IRR of 2.6 ± 0.4 µl O_2 ind.$^{-1}$ d^{-1} (1.2 ± 0.2 µg C ind.$^{-1}$ d^{-1}) and a mass-specific respiration rate (MSRR) of 377.1 ± 28.8 µl O_2 mg^{-1} d^{-1} (165.9 ± 12.8 µg C mg^{-1} d^{-1}). IRR of active ML class species ranged from 3.7 to 24.9 µl O_2 ind.$^{-1}$ d^{-1} (1.6 to 11.0 µg C ind.$^{-1}$ d^{-1}) for *C. brachiatus*, *Calanus chilensis*, *N. minor* and *Euchaeta longicornis.* IRRs for *Euchaeta rimana* and *E. bella* were higher, varying from 29.2 to 63.9 µl O_2 ind.$^{-1}$ d^{-1} (12.8 to 28.1 µg C ind.$^{-1}$ d^{-1}). In contrast, MSRRs of ML class species were lowest in the heaviest species *E. bella*, with 62.3 ± 2.4 µl O_2 mg^{-1} d^{-1} (27.4 ± 1.0 µg C mg^{-1} d^{-1}) and highest in *C. brachiatus* with 216.9–309.1 µl O_2 mg^{-1} d^{-1} (95.4–136.0 µg C mg^{-1} d^{-1}). MSRRs of the 'sluggish' subeucalanid copepods varied from 53.0–72.3 µl O_2 mg^{-1} d^{-1} (23.3–31.8 µg C mg^{-1} d^{-1}) and were in the lower range of MSRRs of the active copepods (Table 1).

MSRRs of *E. inermis* females from the upper 100 m was about twice as high with 31.8 ± 1.1 µl O_2 mg^{-1} d^{-1} (14.0 ± 0.5 µg C mg^{-1} d^{-1}) at 18°C compared to females from depth below 200 m with 14.8 ± 0.7 µl O_2 mg^{-1} d^{-1} (6.5 ± 0.3 µg C mg^{-1} d^{-1}) at 12°C.

3.4. Respiratory carbon demands of copepod communities over depth

Depth-dependent gradients of respiratory carbon demands are shown in Fig. 6 for the northern transect T1 and the southern transect T5, as differences in species composition were most pronounced at these transects.

At transect T1, the respiratory carbon demands of all copepods were 3–9 times higher at the surface layer (0–50 m) than in the depth interval below (50–100 m). The decrease was even more pronounced at

Table 1. Individual (IRR) and mass-specific respiration rates (MSRR) calculated from dry mass (DM) and measured directly (shaded) of dominant copepods from the northern Humboldt Current System off Peru and bulk samples of small copepods (S class). Temperature, depths of origin of the specimens, DM and number (no.) of replicates (via DM) and measurements are given. The total number of individuals used in the measurements is given in brackets. Active and sluggish species are separated by the line. F: female; M: male; C5 and C4: copepodite stages 5 and 4. Mean values ± SD given for n ≥ 3

Species	Stage	Temp. (°C)	Depth (m)	No. (ind.)	DM (µg ind.$^{-1}$)	IRR (µl O_2 ind.$^{-1}$ d^{-1})	MSRR (µl O_2 mg^{-1} d^{-1})
S class	All	20	50–0	13	7 ± 2	2.6 ± 0.4	377.1 ± 28.8
Aetideus armatus	F	20	100–50	20	45 ± 3	8.7 ± 0.3	193.4 ± 3.9
	F	20	100–50	2 (11)	45/103	4.9/2.2	107.8/21.8
Euchirella bella	F	20	100–0	6	1117 ± 118	69.3 ± 4.7	62.3 ± 2.4
	F	20	100–0	6 (6)	1117 ± 118	31.8 ± 7.7	29.0 ± 7.9
Calanus chilensis	F	20	50–0	33	229 ± 22	24.9 ± 1.6	109.1 ± 3.9
	F	20	50–0	7 (24)	197 ± 44	18.2 ± 1.8	95.6 ± 15.7
	F	18	100–50	4 (12)	228 ± 4	12.3 ± 3.7	53.8 ± 15.9
	M	20	50–0	34	160 ± 13	19.8 ± 1.0	123.8 ± 3.5
	M	20	50–0	1 (5)	140	11.4	81.6
	C5	20	50–0	34	134 ± 16	17.6 ± 1.3	132.1 ± 5.4
	C5	20	50–0	6 (34)	157 ± 37	6.4 ± 0.2	44.4 ± 26.0
	C5	18	100–50	15 (71)	142 ± 18	5.3 ± 2.1	32.6 ± 11.1
	C4	20	50–0	30	63 ± 8	10.8 ± 0.9	172.6 ± 7.8
Nannocalanus minor	F	20	50–0	30	96 ± 15	14.2 ± 1.4	148.7 ± 7.7
	M	20	50–0	30	62 ± 11	10.6 ± 1.2	174.6 ± 11.7
	C5	20	50–0	30	62 ± 4	10.8 ± 0.5	172.7 ± 4.2
	C4	20	50–0	20	50 ± 2	9.3 ± 0.2	186.6 ± 2.2
Centropages brachiatus	F	20	100–0	30	33 ± 4	7.1 ± 0.5	216.9 ± 9.0
	F	19	50–0	9 (62)	32 ± 6	6.8 ± 1.4	223.0 ± 69.9
	F	16	100–50	4 (60)	28 ± 4	3.3 ± 1.1	113.7 ± 21.6
	M	20	100–0	30	24 ± 6	5.8 ± 0.9	245.4 ± 21.3
	C5	20	100–0	25	14 ± 3	4.1 ± 0.6	293.7 ± 22.7
	C4	20	100–0	15	12 ± 1	3.7 ± 0.3	309.1 ± 2.3
Euchaeta longicornis	F	20	50–0	20	167 ± 19	20.3 ± 1.6	122.3 ± 5.7
	M	20	50–0	20	186 ± 9	21.8 ± 0.7	117.2 ± 2.1
	C5	20	50–0	20	137 ± 18	17.9 ± 1.5	131.0 ± 5.7
	C4	20	50–0	15	72 ± 18	11.7 ± 1.9	167.0 ± 16.1
Euchaeta rimana	F	20	50–0	30	443 ± 76	38.1 ± 4.4	86.8 ± 6.0
	F	20	70–0	13 (17)	537 ± 95	47.8 ± 6.8	91.2 ± 16.9
	M	20	50–0	20	374 ± 56	34.1 ± 3.5	92.0 ± 5.3
	C5	20	50–0	20	297 ± 66	29.3 ± 4.1	100.3 ± 7.3
	C4	20	50–0	15	150 ± 2	19.0 ± 0.2	126.4 ± 0.6
Eucalanus inermis	F	18	100–0	20	628 ± 103	19.8 ± 2.6	31.8 ± 1.1
	F	16	200–100	3 (3)	393 ± 95	11.4 ± 2.9	35.9 ± 10.6
	F	12	600–200	20	573 ± 130	8.4 ± 1.5	14.8 ± 0.7
	F	12	500–200	7 (9)	596 ± 175	4.6 ± 2.6	7.5 ± 3.7
	M	18	100–0	13	312 ± 102	14.8 ± 3.8	48.1 ± 3.6
	C5	16	200–100	14	164 ± 54	5.3 ± 1.4	32.9 ± 2.6
	C5	16	200–100	4 (7)	303 ± 38	5.4 ± 1.4	21.0 ± 3.5
	C4	18	100–0	10	64 ± 25	4.2 ± 1.4	68.4 ± 6.1
Subeucalanus mucronatus	F	20	50–0	30	192 ± 11	10.1 ± 0.5	53.0 ± 0.6
	M	20	50–0	30	137 ± 3	7.8 ± 0.1	56.9 ± 0.2
	C5	20	50–0	20	95 ± 25	5.8 ± 1.2	61.9 ± 3.0
	C4	20	50–0	15	55 ± 1	3.8 ± 0.1	69.1 ± 0.4
Subeucalanus subtenuis	F	20	50–0	20	109 ± 13	6.5 ± 0.6	59.8 ± 1.7
	M	20	50–0	20	120 ± 8	7.0 ± 0.4	58.6 ± 0.8
	C5	20	50–0	20	58 ± 4	4.0 ± 0.2	68.3 ± 0.9
	C4	20	50–0	15	44 ± 2	3.2 ± 0.1	72.3 ± 0.6

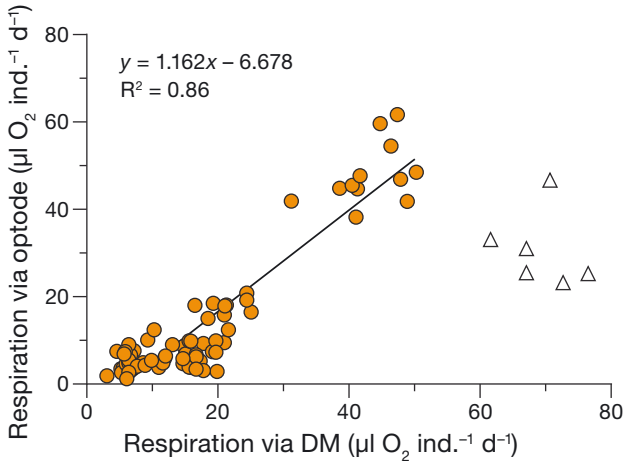

Fig. 5. Relationship between individual respiration rates of copepods (orange circles) determined via optode respirometry and calculated for the respective dry mass (DM) and temperature. *Euchirella bella* (white triangles) was excluded from the regression analyses

transect T5 (Fig. 6). Within the core of the OMZ from 200–500 m, respiratory carbon demands of copepods were lowest compared to all other depth intervals, but generally increased towards the upper boundary of the OMZ at 100–200 m. The decrease in community respiration with depth was attributed to the low biomass of species and lower temperatures at greater depth.

C. chilensis and the S class had the highest community carbon demands (max.: 102 and 47 mg C m^{-2} d^{-2}, respectively) at the coastal stations at transect T1 in all depth intervals (Fig. 6A). Further offshore along transect T1, *N. minor*, *Subeucalanus* spp. and the S class mainly contributed to carbon demand in the upper 100 m, while *C. brachiatus* largely contributed to total carbon demands at transect T5 besides the S class in the upper 50 m (Stn 74: 148 and 373 mg C m^{-2} d^{-2}, respectively). At coastal Stn 67 (T5), the S class had the highest respiratory carbon demand with 183 mg C m^{-2} d^{-2} in the upper 20 m (Fig. 6B).

Considering the low oxygen levels occurring below 50 m throughout the study area, respiration of copepods at greater depths (50–500 m) was most likely severely reduced and metabolic demands at these depths should be used with caution.

3.5. Ingestion and egestion by copepods

The analyses of community ingestion and egestion across the different regions focused on the surface layer where biomass of the species was concentrated, and oxygen levels were generally high and thus had a minor effect on metabolic rates. Ingestion rates of the ML class in the upper 50 m ranged between 14 and 515 mg C m^{-2} d^{-1} in shelf regions and between 11 and 502 mg C m^{-2} d^{-1} in offshore regions. Ingestion rates of these species in shelf regions were lower in the south (14.5–16° S) compared to the north (8.5–9.5° S) and central study area (12° S), whereas offshore ingestion was comparable across the regions from north to south (8.5–16° S). Community ingestion rates (0–50 m) of the S class varied from 100 to 417 mg C m^{-2} d^{-1} in shelf regions and from 177 to 932 mg C m^{-2} d^{-1} in oceanic regions (Table 2).

C. chilensis and *C. brachiatus* were the major contributors to total ingestion of the ML class. Community consumption rates of *C. chilensis* were highest at the northern and central transects T1–T3, where they ranged between 1 and 342 mg C m^{-2} d^{-1} in shelf regions and between 5 and 254 mg C m^{-2} d^{-1} offshore. *C. brachiatus* was mostly absent at transects T1 and T2 but reached high community ingestion rates at shelf regions along transect T3, ranging from 54 to 173 mg C m^{-2} d^{-1}, and offshore in the south at transect T5 with up to 393 mg C m^{-2} d^{-1}. All other ML class species had community ingestion rates of ≤62 mg C m^{-2} d^{-1}.

Community egestion rates are based on the ingestion rates (i.e. 30%) and thus followed the same regional pattern with the same main contributors as for ingestion. Egestion rates varied on average between 3 and 155 mg C m^{-2} d^{-1} for the ML class and between 30 and 280 mg C m^{-2} for the S class (Table 2).

4. DISCUSSION

4.1. Respiration rates as a basis for carbon flow calculations

4.1.1. Choice of methodological approach

Zooplankton respiration is a central component in carbon budgets and carbon fluxes of pelagic ecosystems and can be measured with live animals, enzymatic activities like the electron transport system (Packard et al. 1971) or allometrically from individual DM (Moloney & Field 1989). While direct respiration measurements from live specimens may better reflect the ambient environmental conditions, they are challenging to conduct, especially for species inhabiting greater depths (i.e. obtaining animals in good condition from depth). In contrast, measurements of electron transport system activity and calculations from DM are much easier to handle but rely on assumed parameters for the conversion to respiration rates.

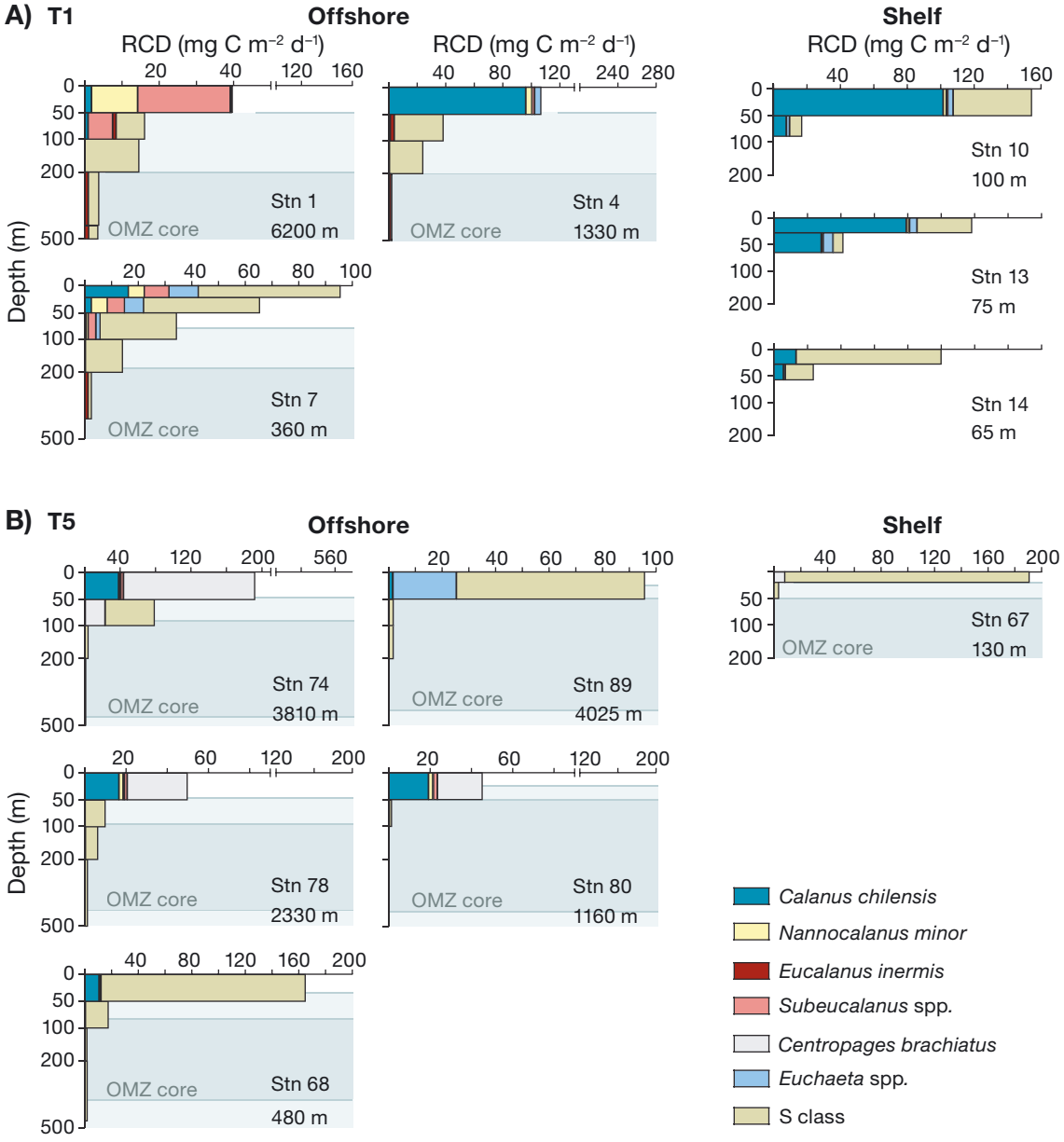

Fig. 6. Respiratory carbon demand (RCD) over depth of the ML class and S class copepods at (A) transect T1 in the north and (B) Transect T5 in the south for offshore and shelf stations. RCD below 500 m was below 3 mg C m^{-2} d^{-1} for both size classes (not shown). Colored area represents the oxygen minimum zone (OMZ) (<45 µmol O_2 l^{-1}) and its anoxic core. Station number and bottom depth are indicated for each station. Note the scale break in some *x*-axes. See Fig. 1 for transect details

In the present study, measurements were carried out with live specimens using optode respirometry. The advantages of this approach over conventional methods such as Winkler titration or Clark electrodes are, for example, the ability to record continuous and non-invasive measurements, and that there is no consumption of oxygen by the optode itself and no use of chemicals (Klimant et al. 1995, Warkentin et al. 2007, Köster et al. 2008). However, these measurements are time consuming, and the handling of specimens due to their fast movements and small body sizes (i.e. availability to obtain sufficient individuals for replicates) can be difficult. To include all dominant copepod species during the cruise, respiration rates were additionally calculated from DM and habitat temperature. This approach has been used for decades and has been continuously developed for copepods and euphausiids (Ikeda et al. 2001, Ikeda 2013, Bode et al. 2018).

Table 2. Community ingestion and egestion rates of medium- to larger-sized (ML class) and small (S class) copepod species in the upper 50 m in shelf (<200 m) and offshore (>200 m) regions for every transect in the northern Humboldt Current System off Peru. Minimum to maximum ranges and average values (in brackets) are given. For the ML class species, stages C4–C6 are included. Ingestion and egestion rates of *Euchaeta* spp. males are excluded since these are assumed to be non-feeding. Calanoid stages C1–C3 are included within the S class. n: number of stations for offshore and shelf regions per transect (see Fig. 3); 0: no occurrence; nd: not determined

	Transect T1		Transect T2		Transect T3		Transect T4		Transect T5		Transect T6	
	Offshore	Shelf	Offshore	Shelf	Offshore	Shelf	Offshore	Shelf	Offshore	Shelf	Offshore	Shelf
Ingestion (mg C m^{-2} d^{-1})	n = 3	n = 3	n = 2	n = 4	n = 2	n = 3	n = 4	n = 1	n = 5	n = 1	n = 5	n = 1
Calanus chilensis	5–240 (98)	48–254 (167)	44/71	2–258 (135)	254/180	1–342 (116)	8–32 (23)	20	4–96 (43)	0	2–43 (21)	3
Nannocalanus minor	11–31 (24)	0–5 (3)	17/21	11–15 (14)	10/2	0	2–21 (13)	0	3–11 (6)	0	1–4 (1)	0
Centropages brachiatus	0	0	0	0–113 (28)	1/1	54–173 (96)	0–43 (18)	131	31–393 (122)	21	0–183 (38)	6
Euchaeta spp.	1–46 (20)	3–11 (7)	25/26	4–11 (6)	13/12	0–1 (<1)	0–9 (4)	2	0–3 (<1)	0	0–1 (<1)	0
Eucalanus inermis	0–<1 (<1)	0	0	0	0	0	0–<1 (<1)	4	0–1 (<1)	0	1–43 (10)	4
Subeucalanus spp.	4–62 (35)	1–2 (1)	0	0–24 (9)	1/1	0	5–35 (19)	4	0–8 (3)	0	0–3 (<1)	1
Total ML class	99–267 (177)	50–269 (178)	86/118	26–341 (183)	279/196	59–515 (212)	16–113 (77)	161	62–502 (174)	21	11–269 (70)	14
S class	241–422 (305)	100–250 (156)	nd	nd	nd	nd	nd	nd	177–932 (429)	417	nd	nd
All copepods	351–690 (482)	297–380 (329)	nd	nd	nd	nd	nd	nd	251–1434 (605)	438	nd	nd
Egestion (mg C m^{-2} d^{-1})												
C. chilensis	2–72 (29)	14–76 (50)	13/21	<1–77 (41)	76/54	<1–103 (35)	2–10 (7)	6	1–29 (13)	0	<1–13 (6)	1
N. minor	3–9 (7)	0–2 (1)	5/6	3–5 (4)	3/<1	0	<1–6 (4)	0	1–3 (2)	0	<1–1 (<1)	0
C. brachiatus	0	0	0	0–34 (8)	<1/<1	16–52 (29)	0–13 (5)	39	9–118 (37)	6	0–55 (11)	2
Euchaeta spp.	<1–14 (6)	1–3 (2)	8/8	1–3 (2)	4/4	<1	0–3 (1)	<1	0–1 (<1)	0	<1	0
E. inermis	<1	0	0	0	0	0	<1	1	<1	0	<1–13 (3)	1
Subeucalanus spp.	1–19 (11)	<1	0	0–7 (3)	<1/<1	0	2–11 (6)	1	0–2 (1)	0	0–1 (<1)	<1
Total ML class	30–80 (53)	15–81 (53)	26/35	8–102 (55)	84/59	18–155 (64)	5–34 (23)	48	19–151 (52)	6	3–81 (21)	4
S class	72–127 (92)	30–75 (47)	nd	nd	nd	nd	nd	nd	53–280 (129)	125	nd	nd
All copepods	105–207 (145)	89–114 (99)	nd	nd	nd	nd	nd	nd	75–430 (182)	131	nd	nd

Measured and calculated respiration rates of this study were significantly positively correlated (r = 0.86), indicating a high reliability of the allometric function from Bode et al. (2018). Furthermore, the consideration of different activity levels by Bode et al. (2018) resulted in a better correlation of measured and calculated respiration rates for the rather sluggish species *Eucalanus inermis*, as well as overall compared to global compilation models by Ikeda et al. (2001, 2007). Previously measured respiration rates of adult *Calanus chilensis* and *E. inermis* (12–18 µl O_2 ind.$^{-1}$ d^{-1}, 16–22°C) sampled at similar regions in the northern HCS (Dagg et al. 1980) are comparable to the measured (11–18 µl O_2 ind.$^{-1}$ d^{-1}, 16–20°C) and calculated (via DM) respiration rates (15–25 µl O_2 ind.$^{-1}$ d^{-1}, 18–20°C) obtained for these species in the present study. However, respiration rates of the largest copepod species, *Euchirella bella*, were ~2 times higher when calculated via DM compared to the measured values. This deviation could indicate that *E. bella* might be able to physiologically reduce its metabolic demand as an adaptation to a life near or within the OMZ, but comparable values for this species are not available in the literature.

4.1.2. Variability of respiration rates

Metabolic rates are influenced by various factors such as body mass, feeding mode, activity levels and migration behavior as well as temperature, oxygen concentration, salinity and pH (Ikeda et al. 2001, Hernández-León & Ikeda 2005b, Paffenhöfer 2006). Differences in temperature and body mass are responsible for up to 95% of the variability in individual respiration rates of zooplankton (Ikeda et al. 2001). Both parameters were implemented in the used approaches (optode respirometry, allometric function). However, the re-creation of ambient oxygen concentrations during experiments is more difficult to implement and was not considered. Yet metabolic suppression under low oxygen concentrations is high (Ekau et al. 2010, Seibel 2011, Kiko & Hauss 2019). Thus, in regions with pronounced OMZs such as the HCS, zooplankton respiration in the core of the OMZ with permanently low oxygen levels reflecting anoxic conditions is emphasized to be severely reduced (Kiko & Hauss 2019). Hence, adaptive processes such as metabolic suppression within the OMZ seem critical to correctly represent the contribution of vertically migrating species to active carbon fluxes and also of deeper-dwelling species to passive fluxes.

The surface layer, where most copepod species occurred and remained during day and night in this study, was generally well ventilated, and thus metabolic suppression should not be a major concern for respiration rates of surface communities.

4.2. Consumption rates of copepod communities off Peru

Feeding rates of copepods as key organisms in marine ecosystems are crucial in order to develop accurate food-web models and carbon budgets. Ingestion rates in this study were assessed by applying an energy budget approach, assuming set values for the RQ as well as the assimilation and growth efficiencies, which vary among studies and thus affect the accuracy of calculated ingestion rates. The applied RQ of 0.82 (Auel & Werner 2003, Schukat et al. 2013, Bode-Dalby et al. 2022) in this study is within the range of RQs (0.61–0.95) calculated for copepods by Mayzaud et al. (2005) and is representative of a mixed diet consisting of proteins, carbohydrates and lipids (Gnaiger 1983). RQs of 0.7 and 0.97 are frequently used for zooplankton species using lipids and carbohydrates as the predominant substrates metabolized, respectively (Omori & Ikeda 1984, Hernández-León & Ikeda 2005a, Almeda et al. 2011) and would increase/decrease the ingestion rates of this study by ~1.2. Furthermore, copepod ingestion is related to food concentration (Kiørboe et al. 1982, Garrido et al. 2013), but this is not considered in energy budgets.

Previously estimated consumption rates of copepods (i.e. *C. chilensis*, *E. inermis* and *Centropages brachiatus*) in the upper 100 m off Peru in shelf and offshore areas (<1–53 mg C m^{-2} d^{-1}; Dagg et al. 1980) were up to ~10 times lower than in the present study for the same species and region (<1–515 mg C m^{-2} d^{-1}). Biomasses of *C. chilensis*, *E. inermis* and *C. brachiatus* were comparable between both studies (Dagg et al. 1980: <1–51 mg DM m^{-3}; this study: <1–77 mg DM m^{-3}). However, individual consumption rates for these species determined via ingested particles (using conversion factors for particle volume and carbon content) were more than 5 times lower in Dagg et al. (1980) than the rates calculated with the energy budget approach in this study. Thus, differences in methodological approaches must also be considered when comparing literature values of zooplankton ingestion rates. Furthermore, the use of the common mesh size of 200 µm for mesozooplankton in this study underestimates the abundance of

the S class species (Turner 2004, Riccardi 2010) and thus their community consumption rates. However, it is still not clear to what extent the numbers of small species are affected, which makes correction of the data difficult.

4.2.1. Regional differences in copepod consumption

Copepod community consumption in shelf regions of upwelling systems is generally much higher than offshore consumption due to the favorable food conditions on the shelf and high abundance of species (Grunewald et al. 2002, Schukat et al. 2013, Bode-Dalby et al. 2022). Our estimates of total consumption at shelf regions (0–50 m, 297–438 mg C m^{-2} d^{-1}) of the northern HCS off Peru are comparable to copepod consumption rates (via gut pigment content and evacuation rates) at shelf regions off central Chile including small- to larger-sized species (0–70 m, 43–553 mg C m^{-2} d^{-1}; Grunewald et al. 2002). However, offshore community ingestion by copepods in the present study is about 4- to 8-fold higher than that reported for the Chilean HCS (via gut pigment; Grunewald et al. 2002) and the northern Benguela upwelling system (via energy budget; Schukat et al. 2013). Offshore copepod abundance, especially of the ML class, was much higher during this study than that reported by Grunewald et al. (2002) and Schukat et al. (2013) as well as offshore SSTs (19–24°C versus 14–17°C), thus causing the higher offshore consumption rates. In the HCS off Peru, large-scale phytoplankton blooms can occur several hundred km offshore (Ayón et al. 2008), sustaining high copepod biomasses. Hence, copepods can provide a high contribution to carbon turnover processes and passive carbon fluxes, not only in coastal areas but also in open ocean regions in the northern HCS off Peru.

Species-specific daily consumption rates for different regions within the Peruvian HCS are available for *C. chilensis*, *E. inermis* and *C. brachiatus* (Dagg et al. 1980). *C. chilensis* is the major consumer in the north between 10 and 11° S and *C. brachiatus* in the south from 15–16° S (Dagg et al. 1980). This pattern agrees well with our study. *C. chilensis* had the highest consumption rates of the ML class in the northern and central region between 8.5 and 12° S, whereas *C. brachiatus* contributed most to the ML class consumption in the south between 14.5 and 16° S. A shift in species composition modulates community consumption as well as the energy and carbon flux of an ecosystem and is associated with local environmental conditions (Manríquez et al. 2009, Medellín-Mora et al. 2016). For instance, small copepods (<1 mm PL) were more abundant during the upwelling season off central and southern Chile, while a more diverse community varying in size ranges occurred during downwelling (Medellín-Mora et al. 2016). The lower SSTs in shelf regions of the southern study area compared to the northern regions during the present study indicate that water was more recently upwelled in the south. The copepod community in this area was dominated by the S class and *C. brachiatus* (i.e. the smallest species of the ML class with a female PL of ~1.2 mm) while the larger species *C. chilensis* (female PL of ~2.2 mm) prevailed in the north. The data from this study may indicate that the smaller copepods of the S class and *C. brachiatus* mainly contribute to carbon turnover rates in newly upwelled water, whereas the contribution of *C. chilensis* and other larger copepods of the ML class to carbon consumption increases during relaxation of upwelling.

4.2.2. Grazing pressure and role of copepod communities in the food web

Copepod community consumption rates can provide estimates of phytoplankton utilization as an essential step to better understand the mechanisms that regulate phytoplankton populations and the downward flux of organic matter in marine ecosystems. Grazing pressure on primary production usually varies greatly within a region. Copepods, including small- and larger-sized species assuming a purely herbivorous diet, graze 1–41% of the daily primary production off Peru (Dagg et al. 1980, Boyd & Smith 1983), 6–25% off northern Chile (González et al. 2000) and 3–46% off central Chile (Grunewald et al. 2002), depending on season and upwelling intensity. Similar ranges of potential grazing impacts occur in other upwelling regions, where 16–44% of primary production is grazed by mesozooplankton off California (Landry et al. 1994) and 3–54% by copepod assemblages in the southern Benguela Current (Verheye et al. 1992). In the present study, the impact of copepod feeding on new primary production including all copepods was variable (0–58%). Grazing impact of the predominantly herbivorous species *C. chilensis* and *Nannocalanus minor* (Massing et al. 2022) accounted for 0–26% of new primary production in the present study. Hence, a crucial amount of new primary production may potentially be ingested by these 2 species. Considering the important role as a carbon source for the Peruvian anchovy (Espinoza

& Bertrand 2008), at least *C. chilensis* fulfills the classical role as a direct link, channeling energy from primary producers to secondary consumers.

In contrast, *C. brachiatus* largely feeds on ciliates and heterotrophic flagellates (Calbet & Saiz 2005, Calbet et al. 2007) and is one of the most abundant copepods in the HCS off Peru during non-El Niño conditions (Gutiérrez et al. 2005). Therefore, this species may play an important role, interlinking the microbial loop with higher trophic levels. Likewise, smaller-sized copepod genera such as the cyclopoids *Oithona* and *Oncaea* or the calanoids *Acartia* and *Paracalanus* are major grazers of heterotrophic protists and phytoplankton (Paffenhöfer 1984, Turner 1986, Saiz & Kiørboe 1995). Their contributions to total copepod biomass, grazing pressure on primary and secondary production, mediated fluxes and trophic interactions in the ocean are usually underestimated (Turner 2004, Roura et al. 2018). Considering an area of 182 000 km^2 from 4 to 18° S for neritic and oceanic regions of the northern HCS off Peru (Chavez & Barber 1987), the S class ingested 9–45 Mt C yr^{-1}, while the ML class ingested 1–34 Mt C yr^{-1}. Estimates for global ingestion of phytoplankton and microzooplankton by small copepods of <2 mm total length, which matches our S class and *C. brachiatus* and *N. minor*, range from 2 to 27 Gt C yr^{-1} (Roura et al. 2018). Considering that the area of the northern HCS off Peru represents 0.05% of the global ocean area (361 × 10^6 km^2; Eakins & Sharman 2010), our calculations are higher (1–80 Gt C yr^{-1}) than the global calculation, most likely reflecting pronounced consumption rates in highly productive regions such as the northern HCS. Roura et al. (2018) emphasized that incorporating the small-size copepod link into biogeochemical models will increase current estimates of biogeochemical fluxes by more than 15%. The results of the present study underline that not only the ML class but also the S class copepods are important components for the calculation and improvement of carbon budget and food-web models in the coastal upwelling system off Peru.

4.3. Contribution of copepods to carbon budgets and export fluxes

4.3.1. Carbon demands of copepod communities

Highly productive surface waters usually result in a considerable transport of biogenic material produced by plankton from the surface layer to depth (Buesseler 1998). The quantity of organic carbon reaching deeper layers is dependent on the efficiency of the biological carbon pump, which is impacted by vertical zonation. ML class species mostly remained in the upper 50 m during night and day in this study. Hence, DVM of the ML class into deeper water layers below 100 m did not occur, and the vertical movement of species was mostly restricted within the upper 50 m during this study. This finding is in accordance with previous studies, which stated that most copepods in the HCS are concentrated in the upper water layers (Judkins 1980, Escribano & Hidalgo 2000, Criales-Hernández et al. 2008, Escribano et al. 2009), most likely due to the exceptionally pronounced OMZ in the HCS (Morales et al. 2010). The vertical zonation resulted in high community respiration rates in the upper 50 m (ML class: 13–108 mg C m^{-2} d^{-1}; S class: 33–169 mg C m^{-2} d^{-1}) which are comparable to those rates estimated for mesozooplankton in the surface layer of the Chilean HCS (Donoso & Escribano 2014, Fernández-Urruzola et al. 2021). A sharp decline in respiratory carbon demands of the ML and S class in the OMZ and below occurred, mainly because of the low biomass. A similar decline in mesozooplankton carbon demands with depth was observed in the Atacama Trench region of Chile (Fernández-Urruzola et al. 2021) and highlights the vital role of copepods in carbon remineralization in the surface mixed layer of the HCS.

4.3.2. Respiratory carbon flux and passive transport of carbon by copepods

The quantitative contributions of upwelling systems to global carbon and nitrogen fluxes are still not fully clarified even though they belong to the most productive ecosystems in the oceans and serve as major sinks or sources of carbon dioxide (Wollast 1988, Brink et al. 1995, Liu et al. 2000). Active carbon flux out of the upper 100–150 m by meso- and macrozooplankton in different regions of the ocean, to upwelling systems (e.g. California Current), to mesotrophic and oligotrophic areas in the Pacific and Atlantic, range from about 2 to 50 mg C m^{-2} d^{-1} (Al-Mutairi & Landry 2001, Hernández-León et al. 2001, Steinberg et al. 2008, Kobari et al. 2013, Stukel et al. 2013). A very high active export of 4417 mg C m^{-2} d^{-1} via DVM into the OMZ (60–600 m) was estimated for the HCS off Chile between 20 and 21° S and was mainly attributed to the krill *Euphausia mucronata* (Escribano et al. 2009). For the same region, a potential active carbon flux to depths below 60 m was calculated for the copepod *E. inermis* with 14 mg C m^{-2}

d^{-1} (Hidalgo et al. 2005). As emphasized by Kiko & Hauss (2019), these carbon fluxes are likely much lower or close to zero, considering the extremely low oxygen concentrations at depths below 60 m in the study area and the pronounced metabolic suppression of zooplankton under such conditions. *E. inermis* was the only species of the ML class that regularly occurred below 100 m in this study, but their similar day–night distribution patterns did not indicate DVM behavior. In contrast, eucalanid copepods were recently classified as strong diel vertical migrants in the HCS of northern Chile (Tutasi & Escribano 2020). However, in that study, both normal and reverse DVM were detected for the eucalanid group. Hence, migration behavior for this group and thus their contribution to active carbon flux is unclear.

The high concentration of the ML and S class copepods during day and night in the surface layer indicates that DVM-mediated active respiratory flux by copepods into the OMZ and deeper layers seems to be of minor importance in the Peruvian upwelling systems or generally in the HCS, considering the extremely low oxygen concentrations in the core of the OMZ (Kiko & Hauss 2019). This observation leads us to the assumption that copepods have a more vital role in the passive flux by the production of fecal material, which is an important component of total particulate organic carbon (POC) flux in the HCS off Chile and in other regions of the oceans (Perissinotto & Pakhomov 1998, Wassmann et al. 2000, Turner 2002, González et al. 2007, Nowicki et al. 2022). In the coastal zone off northern Chile, fecal pellet flux, mainly attributed to euphausiid fecal strings, was variable throughout the year, ranging from ~100 to 800 mg C m^{-2} d^{-1} (González et al. 2007). Egestion of copepods (75–430 mg C m^{-2} d^{-1}), as a measure for fecal pellet production in this study, fell in the range of the fecal pellet flux for the coastal zone off northern Chile. Since fecal pellet production as well as pellet size and stability are dependent on food availability (Dagg & Walser 1986), our calculated egestion rates (i.e. 30% of ingestion regardless of habitat food concentrations; Ikeda & Motoda 1978) are not directly comparable. Nevertheless, they give a potential estimate of egestion rates for the copepod species from the ML and S classes.

Most egested matter from small copepods such as *Acartia* spp. is retained in the water column since small fecal pellets are usually more fragile than larger ones, sink slowly and are rapidly degraded by the microbial system (Olesen et al. 2005, Stamieszkin et al. 2015). Thus, the potential egestion (up to 280 mg C m^{-2} d^{-1}) of the S class in this study is most likely recycled in the surface layer and does not sink to greater depths. In contrast, larger copepod species such as *C. chilensis*, *Subeucalanus* spp., *Euchaeta* spp. and *E. inermis* may produce fecal pellets large and solid enough to sink out of the surface layers into the OMZ due to a higher sinking speed of larger pellets compared to smaller ones (Paffenhöfer & Knowles 1979). Hence, these larger-sized copepods may contribute a crucial amount to the sinking fecal pellet flux in the HCS, whereas fecal pellets of smaller copepod taxa contribute to the recycling of nutrients (Olesen et al. 2005, Stamieszkin et al. 2015). Fecal pellets produced by medium-sized *C. brachiatus* and *N. minor* may contribute equally to both sinking export and recycling processes (Stamieszkin et al. 2015). In accordance, high degradation rates of organic matter in the photic zone off Chile suggest that the bulk of organic matter produced in the system is recycled in the upper water column (Daneri & Pantoja 2007).

We suggest that the high concentration of ML class copepods in the surface layers partly enhances POC fluxes, while the S class can lead to efficient remineralization and recycling of nutrients. Although copepods appear to play a minor role in the active respiratory carbon flux from the surface layer to depth below 100 m of the Peruvian upwelling systems via DVM, their contribution to the recycling of carbon in the surface layer seems to be substantial.

Acknowledgements. We thank the captain and crew of RV 'Maria S. Merian' for their skillful support during the cruise MSM80. We are also grateful to Volker Mohrholz and Toralf Heene for sharing their CTD data. The research activities were granted by the Peruvian Ministry of Production (PRODUCE) under Article 5e of the Supreme Decret No. 019-2021-MINAM. This study was part of the CUSCO project (Coastal Upwelling System in a Changing Ocean) funded by the German Federal Ministry of Education and Research (BMBF, 03F0813C).

LITERATURE CITED

Al-Mutairi H, Landry MR (2001) Active export of carbon and nitrogen at Station ALOHA by diel migrant zooplankton. Deep Sea Res II 48:2083–2103

Alldredge AL (2005) The contribution of discarded appendicularian houses to the flux of particulate organic carbon from oceanic surface waters. In: Gorsky G, Youngbluth MJ, Deibel D (eds) Response of marine ecosystems to global change. Contemporary Publishing International, Paris, p 309–326

Almeda R, Alcaraz M, Calbet A, Saiz E (2011) Metabolic rates and carbon budget of early developmental stages of the marine cyclopoid copepod *Oithona davisae.* Limnol Oceanogr 56:403–414

Antezana T (2009) Species-specific patterns of diel migration into the oxygen minimum zone by euphausiids in the Humboldt Current Ecosystem. Prog Oceanogr 83:228–236

Auel H, Werner I (2003) Feeding, respiration and life history of the hyperiid amphipod *Themisto libellula* in the Arctic marginal ice zone of the Greenland Sea. J Exp Mar Biol Ecol 296:183–197

Ayón P, Criales-Hernández MI, Schwamborn R, Hirche HJ (2008) Zoolankton research off Peru: a review. Prog Oceanogr 79:238–255

Bertrand A, Segura M, Gutiérrez M, Vásquez L (2004) From small-scale habitat loopholes to decadal cycles: a habitat-based hypothesis explaining fluctuation in pelagic fish populations off Peru. Fish Fish 5:296–316

Bode M, Koppelmann R, Teuber L, Hagen W, Auel H (2018) Carbon budgets of mesozooplankton copepod communities in the Eastern Atlantic Ocean — regional and vertical patterns between 24° N and 21° S. Global Biogeochem Cycles 32:840–857

Bode-Dalby M, Würth R, Oliveira LDF, Lamont T and others (2022) Small is beautiful: the important role of small copepods in carbon budgets of the southern Benguela upwelling system. J Plankton Res 2022:fbac061

Boyd CM, Smith SL (1983) Plankton, upwelling and coastally trapped waves off Peru. Deep Sea Res 30:723–742

Boyd CM, Smith SL, Cowles TJ (1980) Grazing patterns of copepods in the upwelling system off Peru. Limnol Oceanogr 25:583–596

Boyd PW, Gall MP, Silver MW, Coale SL, Bidigare RR, Bishop JKB (2008) Quantifying the surface–subsurface biogeochemical coupling during the VERTIGO ALOHA and K2 studies. Deep Sea Res II 55:1578–1593

Brink KH, Abrantes FF, Bernal PA, Dugdale RC and others (1995) How do coastal upwelling systems operate as integrated physical, chemical, and biological systems and influence the geological report? The role of physical processes in defining the spatial structures and biological and chemical variables. In: Summerhayes CP, Emeis KC, Angel MV, Smith RL, Zeitzschel B (eds) Upwelling in the ocean: modern processes and ancient records. Environmental Sciences Research Report No. 18. John Wiley and Sons, Chichester, p 1585–1586

Brown JH, Gillooly JF, Allen AP, Savage VM, West GB (2004) Toward a metabolic theory of ecology. Ecology 85: 1771–1789

Buesseler KO (1998) The decoupling of production and particulate export in the surface ocean. Global Biogeochem Cycles 12:297–310

Calbet A, Saiz E (2005) The ciliate–copepod link in marine ecosystems. Aquat Microb Ecol 38:157–167

Calbet A, Carlotti F, Gaudy R (2007) The feeding ecology of the copepod *Centropages typicus* (Krøyer). Prog Oceanogr 72:137–150

Carr ME (2002) Estimation of potential productivity in Eastern Boundary Currents using remote sensing. Deep Sea Res II 49:59–80

Castro LR, Bernal PA, González HE (1991) Vertical distribution of copepods and the utilization of the chlorophyll *a*-rich layer within Concepcion Bay, Chile. Estuar Coast Shelf Sci 32:243–256

Castro LR, Troncoso VA, Figueroa DR (2007) Fine-scale vertical distribution of coastal and offshore copepods in the Golfo de Arauco, central Chile, during the upwelling season. Prog Oceanogr 75:486–500

Chavez FP, Barber RT (1987) An estimate of new production in the equatorial Pacific. Deep Sea Res I 34:1229–1243

Chavez FP, Messié M (2009) A comparison of Eastern Boundary Upwelling Ecosystems. Prog Oceanogr 83:80–96

Chavez FP, Bertrand A, Guevara-Carrasco R, Soler P, Csirke J (2008) The northern Humboldt Current System: brief history, present status and a view towards the future. Prog Oceanogr 79:95–105

Criales-Hernández MI, Schwamborn R, Graco M, Ayón P, Hirche HJ, Wolff M (2008) Zooplankton vertical distribution and migration off central Peru in relation to the oxygen minimum layer. Helgol Mar Res 62(Suppl 1):85–100

Dagg MJ, Walser EW Jr (1986) The effect of food concentration on fecal pellet size in marine copepods. Limnol Oceanogr 31:1066–1071

Dagg M, Cowles T, Whitledge T, Smith S, Howe S, Judkins D (1980) Grazing and excretion by zooplankton in the Peru upwelling system during April 1977. Deep Sea Res 27:43–59

Daneri G, Pantoja S (2007) Mineralization of organic matter: the importance of pelagic bacterioplankton in the Humboldt Current System off Chile. COPAS Newsletter 13

Donoso K, Escribano R (2014) Mass-specific respiration of mesozooplankton and its role in the maintenance of an oxygen-deficient ecological barrier (BEDOX) in the upwelling zone off Chile upon presence of a shallow oxygen minimum zone. J Mar Syst 129:166–177

Eakins BW, Sharman GF (2010) Volumes of the world's oceans from ETOPO1. NOAA National Geophysical Data Center, Boulder, CO

Ekau W, Auel H, Pörtner HO, Gilbert D (2010) Impacts of hypoxia on the structure and processes in pelagic communities (zooplankton, macro-invertebrates and fish). Biogeosciences 7:1669–1699

Escribano R (2006) Zooplankton interactions with the oxygen minimum zone in the eastern South Pacific. Suplemento Gayana 70:19–21

Escribano R, Hidalgo P (2000) Spatial distribution of copepods in the north of the Humboldt Current region off Chile during coastal upwelling. J Mar Biol Assoc UK 80:283–290

Escribano R, Hidalgo P, Krautz C (2009) Zooplankton associated with the oxygen minimum zone system in the northern upwelling region off Chile during March 2000. Deep Sea Res II 56:1083–1094

Espinoza P, Bertrand A (2008) Revisiting Peruvian anchovy (*Engraulis ringens*) trophodynamics provides a new vision of the Humboldt Current System. Prog Oceanogr 79:215–227

Fernández-Urruzola I, Ulloa O, Glud RN, Pinkerton MH, Schneider W, Wenzhöfer F, Escribano R (2021) Plankton respiration in the Atacama Trench region: implications for particulate organic carbon flux into the hadal realm. Limnol Oceanogr 66:3134–3148

Fuenzalida R, Schneider W, Garces-Vargas J, Bravo L, Lange C (2009) Vertical and horizontal extension of the oxygen minimum zone in the eastern South Pacific Ocean. Deep Sea Res II 56:992–1003

Garrido S, Cruz J, Santos AMP, Ré P, Saiz E (2013) Effects of temperature, food type and food concentration on the grazing of the calanoid copepod *Centropages chierchiae*. J Plankton Res 35:843–854

Gnaiger E (1983) Calculation of energetic and biochemical equivalents of respiratory oxygen consumption. In: Gnaiger E, Forstner H (eds) Polarographic oxygen sensors. Springer, Berlin, p 337–345

González HE, Ortiz VC, Sobarzo M (2000) The role of faecal material in the particulate organic carbon flux in the northern Humboldt Current, Chile (23° S), before and during the 1997–1998 El Niño. J Plankton Res 22:499–529

González HE, Menschel E, Aparicio C, Barría C (2007) Spa-

tial and temporal variability of microplankton and detritus, and their export to the shelf sediments in the upwelling area off Concepción, Chile (~36° S), during 2002–2005. Prog Oceanogr 75:435–451

Grunewald AC, Morales CE, González HE, Sylvester C, Castro LR (2002) Grazing impact of copepod assemblages and gravitational flux in coastal and oceanic waters off central Chile during two contrasting seasons. J Plankton Res 24:55–67

Gutiérrez D, Aronés K, Chang F, Quipúzcoa L, Villanueva P (2005) Impacto de la variación oceanográfica estacional e interanual sobre los ensambles de microfitoplancton, mesozooplancton, ictioplancton y macrozoobentos de dos áreas costeras del norte del Peru entre 1994 y 2002. Bol Inst Mar Peru 22:1–60

Hansen FC, Cloete RR, Verheye HM (2005) Seasonal and spatial variability of dominant copepods along a transect off Walvis Bay (23° S), Namibia. Afr J Mar Sci 27:55–63

Hernández-León S, Ikeda T (2005a) A global assessment of mesozooplankton respiration in the ocean. J Plankton Res 27:153–158

Hernández-León S, Ikeda T (2005b) Zooplankton respiration. In: del Giorgio PA, Williams PJ (eds) Respiration in aquatic ecosystems. Oxford University Press, Oxford, p 57–82

Hernández-León S, Gómez M, Pagazaurtundua M, Portillo-Hahnefeld A, Montero I, Almeida C (2001) Vertical distribution of zooplankton in Canary Island waters: implications for export flux. Deep Sea Res I 48:1071–1092

Hernández-León S, Olivar MP, Fernández de Puelles ML, Bode A and others (2019) Zooplankton and micronecton active flux across the tropical Atlantic Ocean. Front Mar Sci 6:535

Hidalgo P, Escribano R, Morales CE (2005) Ontogenetic vertical distribution and diel migration of the copepod *Eucalanus inermis* in the oxygen minimum zone off northern Chile (20–21° S). J Plankton Res 27:519–529

Ikeda T (2013) Respiration and ammonia excretion of euphausiid crustaceans: synthesis toward a global-bathymetric model. Mar Biol 160:251–262

Ikeda T, Motoda S (1978) Estimated zooplankton production and their ammonia excretion in the Kuroshio and adjacent seas. Fish Bull 76:357–366

Ikeda T, Torres JJ, Hernández-León S, Geiger SP (2000) Oxygen consumption as an index of metabolism. In: Harris RP, Wiebe PH, Lenz J, Skjøldal HR, Huntley M (eds) ICES zooplankton methodology manual. Academic Press, London, p 455–458

Ikeda T, Kanno Y, Ozaki K, Shinada A (2001) Metabolic rates of epipelagic marine copepods as a function of body mass and temperature. Mar Biol 139:587–596

Ikeda T, Sano F, Yamaguchi A (2007) Respiration in marine pelagic copepods: a global-bathymetric model. Mar Ecol Prog Ser 339:215–219

Judkins DC (1980) Vertical distribution of zooplankton in relation to the oxygen minimum off Peru. Deep Sea Res 27:475–487

Kiko R, Hauss H (2019) On the estimation of zooplankton-mediated active fluxes in oxygen minimum zone regions. Front Mar Sci 6:741

Kiko R, Hauss H, Buchholz F, Melzner F (2016) Ammonium excretion and oxygen respiration of tropical copepods and euphausiids exposed to oxygen minimum zone conditions. Biogeosciences 13:2241–2255

Kiørboe T, Møhlenberg F, Nicolajsen H (1982) Ingestion rate and gut clearance in the planktonic copepod *Centropages hamatus* (Lilljeborg) in relation to food concentration and temperature. Ophelia 21:181–194

Klimant I, Meyer V, Kühl M (1995) Fiber-optic oxygen microsensors, a new tool in aquatic biology. Limnol Oceanogr 40:1159–1165

Kobari T, Kitamura M, Minowa M, Isami H and others (2013) Impacts of the wintertime mesozooplankton community to downward carbon flux in the subarctic and subtropical Pacific Oceans. Deep Sea Res I 81:78–88

Koski M, Valencia B, Newstead R, Thiele C (2020) The missing piece of the upper mesopelagic carbon budget? Biomass, vertical distribution and feeding of aggregate-associated copepods at the PAP site. Prog Oceanogr 181: 102243

Köster M, Krause C, Paffenhöfer GA (2008) Time-series measurements of oxygen consumption of copepod nauplii. Mar Ecol Prog Ser 353:157–164

Landry MR, Lorenzen CJ, Peterson WK (1994) Mesozooplankton grazing in the Southern California Bight. II. Grazing impact and particulate flux. Mar Ecol Prog Ser 115:73–85

Liu KK, Iseki K, Chao SY (2000) Continental margin carbon fluxes. In: Hanson RB, Ducklow HW, Field J (eds) The changing global ocean carbon cycle. International geosphere–biosphere programme book series 5. Cambridge University Press, Cambridge, p 187–239

Longhurst AR, Bedo AW, Harrison WG, Head EJH, Sameoto DD (1990) Vertical flux of respiratory carbon by oceanic diel migrant biota. Deep Sea Res 37:685–694

Manríquez K, Escribano R, Hidalgo P (2009) The influence of coastal upwelling on the mesozooplankton community structure in the coastal zone off central/southern Chile as assessed by automated image analysis. J Plankton Res 31:1075–1088

Massing JC, Schukat A, Auel H, Auch D and others (2022) Toward a solution of the 'Peruvian puzzle': pelagic food-web structure and trophic interactions in the northern Humboldt Current Upwelling System off Peru. Front Mar Sci 8:759603

Mayzaud P, Boutoute M, Gasparini S, Mousseau L, Lefevre D (2005) Respiration in marine zooplankton — the other side of the coin: CO_2 production. Limnol Oceanogr 50:291–298

Medellín-Mora J, Escribano R, Schneider W (2016) Community response of zooplankton to oceanographic changes (2002–2012) in the central/southern upwelling system of Chile. Prog Oceanogr 142:17–29

Moloney CL, Field JG (1989) General allometric equations for rates of nutrient uptake, ingestion, and respiration in plankton organisms. Limnol Oceanogr 34:1290–1299

Montecino V, Lange CB (2009) The Humboldt Current System: ecosystem components and processes, fisheries, and sediment studies. Prog Oceanogr 83:65–79

Morales CE, Torreblanca ML, Hormazabal S, Correa-Ramirez M, Nunez S, Hidalgo P (2010) Mesoscale structure of copepod assemblages in the coastal transition zone and oceanic waters off central-southern Chile. Prog Oceanogr 84:158–173

Motoda S (1959) Devices of simple plankton apparatus. Mem Fac Fish Hokkaido Univ 7:73–94

Nowicki M, DeVries T, Siegel DA (2022) Quantifying the carbon export and sequestration pathways of the ocean's biological carbon pump. Glob Biogeochem Cycles 36: e2021GB007083

Olesen M, Strake S, Andrushaitis A (2005) Egestion of non-pellet-bound fecal material from the copepod *Acartia tonsa*: implication for vertical flux and degradation. Mar Ecol Prog Ser 293:131–142

Omori M, Ikeda T (1984) Methods in marine zooplankton ecology. John Wiley and Sons, New York, NY

Packard TT, Healy ML, Richards FA (1971) Vertical distribution of activity of respiratory electron transport system in marine plankton. Limnol Oceanogr 16:60–70

Packard TT, Healy ML, Richards FA (1971) Vertical distribution of activity of respiratory electron transport system in marine plankton. Limnol Oceanogr 16:60–70

Paffenhöfer GA (1984) Food ingestion by the marine planktonic copepod *Paracalanus* in relation to abundance and size distribution of food. Mar Biol 80:323–333

Paffenhöfer GA (2006) Oxygen consumption in relation to motion of marine planktonic copepods. Mar Ecol Prog Ser 317:187–192

Paffenhöfer GA, Knowles SC (1979) Ecological implications of fecal pellet size, production and consumption by copepods. J Mar Res 37:35–49

Pakhomov EA, Froneman PW, Kuun PJ, Balarin M (1999) Feeding dynamics and respiration of the bottom-dwelling caridean shrimp *Nauticaris marionis* Bate, 1888 (Crustacea: Decapoda) in the vicinity of Marion Island (Southern Ocean). Polar Biol 21:112–121

Perissinotto R, Pakhomov EA (1998) Contribution of salps to carbon flux of marginal ice zone of the Lazarev Sea, Southern Ocean. Mar Biol 131:25–32

Peterson WT, Arcos DF, McManus GB, Dam H, Bellantoni D, Johnson T, Tiselius P (1988) The nearshore zone during coastal upwelling: daily variability and coupling between primary and secondary production off central Chile. Prog Oceanogr 20:1–40

Riccardi N (2010) Selectivity of plankton nets over mesozooplankton taxa: implications for abundance, biomass and diversity estimation. J Limnol 69:287–296

Roura Á, Strugnell JM, Guerra Á, González ÁF, Richardson AJ (2018) Small copepods could channel missing carbon through metazoan predation. Ecol Evol 8:10868–10878

Saiz E, Kiørboe T (1995) Predatory and suspension feeding of the copepod *Acartia tonsa* in turbulent environments. Mar Ecol Prog Ser 122:147–158

Schukat A, Teuber L, Hagen W, Wasmund N, Auel H (2013) Energetics and carbon budgets of dominant calanoid copepods in the northern Benguela upwelling system. J Exp Mar Biol Ecol 442:1–9

Schukat A, Hagen W, Dorschner S, Correa Acosta J, Pinedo Arteaga EL, Ayón P, Auel H (2021) Zooplankton ecological traits maximize the trophic transfer efficiency of the Humboldt Current upwelling system. Prog Oceanogr 193: 102551

Schukat A, Bode-Dalby M, Massing JC, Hagen W, Auel H (2022) Respiration, ingestion and egestion rates of copepods from the northern Humboldt Current System off Peru during Maria S. Merian cruise MSM80. PANGAEA, doi.org/10.1594/PANGAEA.949569

Seibel BA (2011) Critical oxygen levels and metabolic suppression in oceanic oxygen minimum zones. J Exp Biol 214:326–336

Stamieszkin K, Pershing AJ, Record NR, Pilskaln CH, Dam HG, Feinberg LR (2015) Size as the master trait in modeled copepod fecal pellet carbon flux. Limnol Oceanogr 60:2090–2107

Steedman HF (ed) (1976) Zooplankton fixation and preservation. Monographs on Oceanographic Methodology No. 4. UNESCO Press, Paris

Steinberg DK, Landry MR (2017) Zooplankton and the ocean carbon cycle. Annu Rev Mar Sci 9:413–444

Steinberg DK, Van Mooy BAS, Buesseler KO, Boyd PW, Kobari T, Karl DM (2008) Bacterial vs. zooplankton control of sinking particle flux in the ocean's twilight zone. Limnol Oceanogr 53:1327–1338

Stukel MR, Ohman MD, Benitez-Nelson CR, Landry MR (2013) Contributions of mesozooplankton to vertical carbon export in a coastal upwelling system. Mar Ecol Prog Ser 491:47–65

Teuber L, Hagen W, Bode M, Auel H (2019) Who is who in the tropical Atlantic? Functional traits, ecophysiological adaptations and life strategies in tropical calanoid copepods. Prog Oceanogr 171:128–135

Turner JT (1986) Zooplankton feeding ecology: contents of fecal pellets of the cyclopoid copepods *Oncaea venusta*, *Corycaeus amazonicus*, *Oithona plumifera*, and *O. simplex* from the Northern Gulf of Mexico. Mar Ecol 7: 289–302

Turner JT (2002) Zooplankton fecal pellets, marine snow and sinking phytoplankton blooms. Aquat Microb Ecol 27:57–102

Turner JT (2004) The importance of small planktonic copepods and their roles in pelagic marine food webs. Zool Stud 43:255–266

Tutasi P, Escribano R (2020) Zooplankton diel vertical migration and downward C flux into the oxygen minimum zone in the highly productive upwelling region off northern Chile. Biogeosciences 17:455–473

Vargas CA, González HE (2004) Plankton community structure and carbon cycling in a coastal upwelling system. I. Bacteria, microprotozoans and phytoplankton in the diet of copepods and appendicularians. Aquat Microb Ecol 34:151–164

Vargas CA, Tönnesson K, Sell A, Maar M and others (2002) Importance of copepods versus appendicularians in vertical carbon fluxes in a Swedish fjord. Mar Ecol Prog Ser 241:125–138

Verheye HM, Hutchings L, Huggett JA, Painting SJ (1992) Mesozooplankton dynamics in the Benguela ecosystem, with emphasis on the herbivorous copepods. S Afr J Mar Sci 12:561–584

Warkentin M, Freese HM, Karsten U, Schumann R (2007) New and fast method to quantify respiration rates of bacterial and plankton communities in freshwater ecosystems by using optical oxygen sensor spots. Appl Environ Microbiol 73:6722–6729

Wassmann P, Ypma JE, Tselepides A (2000) Vertical flux of faecal pellets and microplankton on the shelf of the oligotrophic Cretan Sea (NE Mediterranean Sea). Prog Oceanogr 46:241–258

Wollast R (1988) Evaluation and comparison of the global carbon cycle in the coastal zone and in the open ocean. In: Brink KH, Robinson A (eds) The sea. John Wiley and Sons, New York, NY, p 213–252

Yen J (1988) Directionality and swimming speeds in predator–prey and male–female interactions of *Euchaeta rimana*, a subtropical marine copepod. Bull Mar Sci 43:395–403

Yen J (1991) Predatory feeding behavior of an Antarctic marine copepod, *Euchaeta antarctica.* Polar Res 10:433–442

Editorial responsibility: Marsh Youngbluth, Fort Pierce, Florida, USA
Reviewed by: K. Cook and 5 anonymous referees

Submitted: August 11, 2022
Accepted: September 26, 2023
Proofs received from author(s): November 30, 2023